Earth Surface Processes and Landforms
Earth Surf. Process. Landforms **30**, 1025–1038 (2005)
Published online in Wiley InterScience (www.interscience.wiley.com). **DOI:** 10.1002/esp.1260

Erosion rates over millennial and decadal timescales at Caspar Creek and Redwood Creek, Northern California Coast Ranges

Ken L. Ferrier,[1]* James W. Kirchner[1] and Robert C. Finkel[2]
[1] *Department of Earth and Planetary Science, University of California, Berkeley, California 94720-4767, USA*
[2] *Center for Accelerator Mass Spectrometry, Lawrence Livermore National Laboratory, Livermore, California 94550, USA*

**Correspondence to: K. L. Ferrier, Department of Earth and Planetary Science, University of California, Berkeley, California 94720-4767, USA. E-mail: ferrier@eps.berkeley.edu*

Received 1 September 2004; Revised 28 February 2005; Accepted 17 March 2005

Abstract

Comparing millennial-scale denudation rates from cosmogenic nuclides with decadal-scale sediment yields can shed light on erosional processes and on the effects of land use on sediment delivery to streams. Detailed measurements of sediment fluxes in the Northern California Coast Ranges at Caspar Creek and Redwood Creek have provided estimates of physical erosion rates since 1963 and 1971, respectively. We used cosmogenic ^{10}Be to measure millennial-scale denudation rates averaged over 1400–8700 years at six catchments in Caspar Creek and four catchments in Redwood Creek. Our ^{10}Be measurements at Caspar Creek imply denudation rates that are nearly spatially uniform across the entire catchment and average $0{\cdot}09 \pm 0{\cdot}02$ mm a^{-1}. These millennial-scale rates implied by cosmogenic ^{10}Be are faster than physical erosion rates of $0{\cdot}005 \pm 0{\cdot}001$ mm a^{-1} to $0{\cdot}046 \pm 0{\cdot}007$ mm a^{-1} inferred from sediment flux measurements over the past few decades in the same catchments. At Redwood Creek, our cosmogenic ^{10}Be measurements imply millennial-scale denudation rates that vary across the catchment from $0{\cdot}14 \pm 0{\cdot}03$ mm a^{-1} to $0{\cdot}44 \pm 0{\cdot}09$ mm a^{-1}, in contrast to physical erosion rates ranging from $0{\cdot}038 \pm 0{\cdot}011$ mm a^{-1} to $0{\cdot}48 \pm 0{\cdot}09$ mm a^{-1} derived from sediment flux measurements made over the past few decades at the same catchments. The decadal-scale and millennial-scale measurements tend to differ most at the smallest tributaries, but differ by less than a factor of three for the Caspar Creek and Redwood Creek catchments as a whole. These measurements suggest that denudation rates at Caspar Creek are slower than rock uplift rates of 0·3–0·4 mm a^{-1}, implying that Caspar Creek is not in topographic steady state. Copyright © 2005 John Wiley & Sons, Ltd.

Keywords: erosion rate; cosmogenic ^{10}Be; Northern California Coast Ranges

Introduction

Erosion rate measurements are essential for modelling landscape evolution, quantifying soil formation rates (e.g. Heimsath *et al*., 1997), determining patterns of chemical weathering (e.g. Riebe *et al*., 2003), and understanding how sediment loading affects stream ecosystems. Comparing recent sediment yields to long-term 'background' rates of erosion can shed light on erosional processes and on the effects of land use on sediment delivery to streams. Cosmogenic nuclides such as ^{10}Be in stream sediments can be used to estimate whole-catchment denudation rates averaged over thousands of years, a timescale that is unobservable by conventional methods. These millennial-scale denudation rates can provide useful reference points for quantifying the effects of land use practices on sediment yields (e.g. Brown *et al*., 1998; Hewawasam *et al*., 2003).

In this study we focus on two catchments in the Northern California Coast Ranges, Caspar Creek and Redwood Creek (Figure 1), where stream sediment fluxes have been measured for several decades. The Northern California Coast Ranges are a rapidly evolving mountain range, undergoing rapid erosion under moderate-to-high rates of uplift associated with migration of the Mendocino Triple Junction (e.g. Merritts and Vincent, 1989). The old-growth coastal redwood (*Sequoia sempervirens*) forests in the Coast Ranges have largely been harvested over the past two centuries, and much research has been done at Caspar Creek and Redwood Creek to assess the effects of timber harvesting on stream ecology and stream sediment loading (e.g. Lewis, 1998; Nolan and Janda, 1995; Marron *et al*., 1995; Madej, 2001).

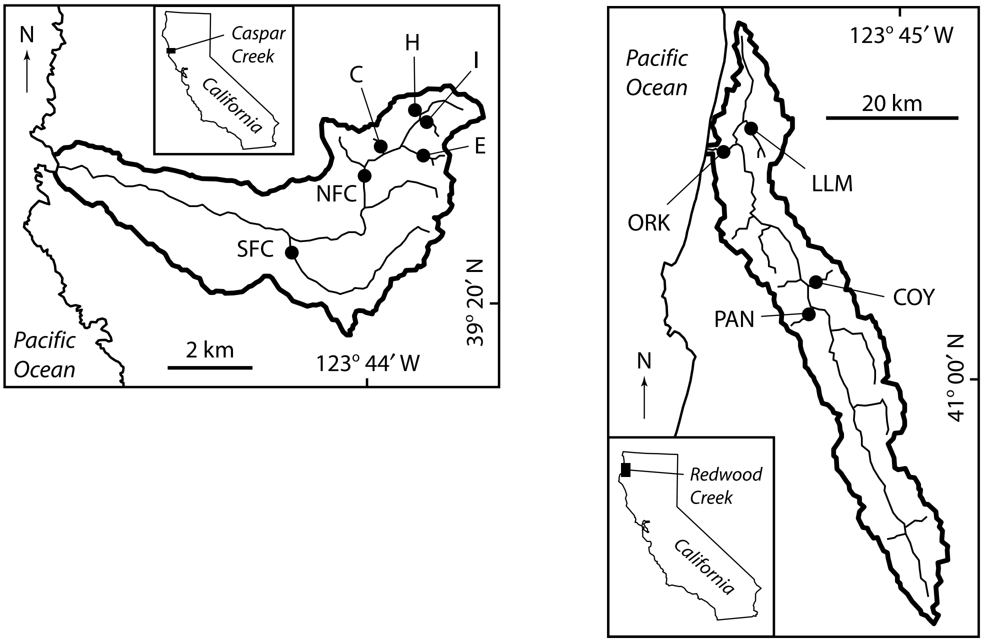

Figure 1. Sample sites for ^{10}Be in alluvial stream sediment at Caspar Creek and Redwood Creek, Northern California. Caspar Creek site labels: NFC, North Fork Caspar Creek; SFC, South Fork Caspar Creek; C, Carlson; E, Eagle; H, Henningson; I, Iverson. Redwood Creek site labels: COY, Coyote Creek; LLM, Little Lost Man Creek; ORK, Redwood Creek at Orick; PAN, Panther Creek. The Grogan Fault closely follows the main stem of Redwood Creek, and separates the Redwood Creek Schist to the west from weak Franciscan sandstones and mudstones to the east (Harden *et al.*, 1981). Note different map scales.

Ongoing measurements of stream sediment fluxes at Caspar Creek and Redwood Creek since 1962 and 1971, respectively, have provided some of the longest and most detailed sediment yield records in the Pacific Northwest. Using our measurements of cosmogenic ^{10}Be in stream sediment, we calculated denudation rates averaged over the past several thousand years at ten locations within these catchments, and compared these rates to sediment yields measured over the past few decades. Our results imply that, at individual subcatchments, decadal-scale sediment yields at Caspar Creek are as much as 16 times lower than millennial-scale denudation rates, and at Redwood Creek, sediment yields over the past few decades differ from millennial-scale average rates of sediment production by less than a factor of four. However, for Caspar Creek and Redwood Creek as a whole, sediment yields over the past few decades are generally consistent, within a factor of three, with millennial-scale rates of sediment production estimated from cosmogenic ^{10}Be.

Field Sites

Caspar Creek

Caspar Creek is a small (*c*. 9 km^2) experimental catchment in Northern California (39°21′ N, 123°44′ W; Figure 1) that drains into the Pacific Ocean through a series of incised, uplifted marine terraces. Steep, soil-mantled hillslopes within the catchment reach a maximum elevation of 320 m, and are underlain by the Coastal Belt Franciscan formation (Jennings and Strand, 1960), a lithology composed of greywacke and feldspathic sandstone, with lesser amounts of siltstone, mudstone and conglomerate. Soils are highly permeable clay loams 1–2 m in depth (Henry, 1998), allowing rapid subsurface storm flow. The climate is Mediterranean, with mild fluctuations around a mean annual temperature of 12 °C, and 90 per cent of the mean annual precipitation of *c*. 1200 mm falling between November and May (RSL website, 2004). Stream sediment has been monitored intensively at Caspar Creek since 1962 under the California Department of Forestry and Fire Protection and the USDA Forest Service (Henry, 1998).

Redwood Creek

Redwood Creek flows roughly northwest in a steep narrow catchment 720 km^2 in size, discharging into the Pacific Ocean at about 41°18′ N, 124°6′ W (Figure 1). The main stem of Redwood Creek closely follows the Grogan Fault, which separates the Redwood Creek Schist to the west from weak, unmetamorphosed Franciscan sandstones and mudstones to the east (Harden *et al*., 1981). Like Caspar Creek, the climate in the Redwood Creek basin is Mediterranean, with *c*. 90 per cent of the precipitation falling from October to April. Mean annual precipitation is *c*. 1700 mm near the mouth of Redwood Creek at Prairie Creek Park in Orick (WRCC website, 2004) and may be as high as 2540 mm in the headwaters (Iwatsubo *et al*., 1975). The maximum elevation within the basin is 1615 m, and at higher elevations some of the winter precipitation falls as snow. Sediment monitoring began at Orick near the mouth of Redwood Creek under the USGS in 1971, and has since expanded to include suspended sediment measurements at many gauging stations within the catchment. Suspended sediment monitoring is now under the supervision of Redwood National Park and Redwood State Park.

Methodology

Beryllium-10-derived denudation rates and assumptions

Concentrations of ^{10}Be in quartz grains in stream sediment can be used to calculate spatially averaged denudation rates over the upstream basin, if it can be assumed that the sampled sediment is representative of all sediment delivered to the stream, and if the mean residence time of sediment in storage and transport is much shorter than the erosional timescale $\Lambda\ \rho_{rock}^{-1}\ \varepsilon^{-1}$, where ρ_{rock} is the bedrock density, ε is the erosion rate, and Λ is the mean penetration depth of cosmogenic neutrons expressed as mass per unit area, in order to be invariant for materials of differing densities (Brown *et al*., 1995; Bierman and Steig, 1996; Granger *et al*., 1996). In order to obtain samples that are representative of sediment delivered to the stream, we collected well-mixed, recently mobilized sediment in stream channels. We do not know the storage history of the sediment in our samples, but the small volumes of sediment stored in the river networks suggest that mean storage and transport timescales are much shorter than the erosional timescale. Channel-stored sediment was estimated to be $1{\cdot}6 \times 10^3$ tons at the North Fork of Caspar Creek (Napolitano, 1998), $4{\cdot}3 \times 10^7$ tons at Redwood Creek (Madej, 1995), and $2{\cdot}2 \times 10^4$ tons at Coyote Creek, a tributary of Redwood Creek (Pitlick, 1995). At the denudation rates measured in our study, the mean residence times of sediment in storage at these sites are 1–52 years. This would add <350 atoms of ^{10}Be g^{-1} to the samples, which is far less than our measured ^{10}Be concentrations (Table I).

Table I. Sample basin characteristics, measured ^{10}Be concentrations, and calculated denudation rates

Catchment	Gauging station latitude, longitude (deg N, deg W)	Basin area (km^2)	Mean altitude (m)*	Mean hillslope gradient*	^{10}Be conc. (10^5 at g^{-1}) (mean ± s.e.)	Cosmogenic denudation rate (mm a^{-1}) (mean ± s.e.)	Time scale (a)†
Caspar Creek							
North Fork	39·36, 123·73	4·73	211	0·36	0·316 ± 0·020	0·107 ± 0·020	5540
South Fork	39·34, 123·75	4·24	170	0·33	0·449 ± 0·036	0·068 ± 0·013	8700
Carlson	39·37, 123·73	0·26	229	0·37	0·339 ± 0·022	0·101 ± 0·019	5856
Eagle	39·37, 123·72	0·27	242	0·38	0·487 ± 0·031	0·072 ± 0·014	8178
Henningson	39·36, 123·72	0·39	232	0·35	0·334 ± 0·021	0·103 ± 0·020	5737
Iverson	39·36, 123·72	0·21	226	0·34	0·439 ± 0·048	0·080 ± 0·017	7436
Redwood Creek							
Redwood Creek at Orick	41·30, 124·05	720	567	0·35	0·106 ± 0·008	0·438 ± 0·088	1353
Coyote Creek	41·12, 123·91	20·18	596	0·34	0·251 ± 0·025	0·184 ± 0·040	3216
Little Lost Man Creek	41·32, 124·02	8·96	391	0·29	0·294 ± 0·023	0·138 ± 0·028	4308
Panther Creek	41·09, 123·91	15·7	489	0·34	0·190 ± 0·012	0·225 ± 0·044	2639

* Mean altitudes and mean hillslope gradients were determined from 10 m SDTS (Spatial Data Transfer Standard) digital elevation data.

† Erosional timescales are calculated as $\Lambda\ \rho_{rock}^{-1}\ \varepsilon^{-1}$, where Λ is the mean penetration depth of cosmogenic neutrons (160 g cm^{-2}), ρ_{rock} is the bedrock density (2·7 g cm^{-3}), and ε is the cosmogenic denudation rate.

Table II. Summary of parameters used to calculate denudation rate ε in Equation 1

Parameter	Value	Description	Source
In Equation 1			
τ	2·18 ± 0·09 Ma	Meanlife of ^{10}Be	Middleton *et al.* (1993)
ρ	2·7 g cm^{-3}	Bedrock density	Assumed
Λ	160 ± 10 g cm^{-2}	Neutron penetration depth	Masarik and Reedy (1995)
L_1	738·6 g cm^{-2}	Muon penetration depth	Granger and Smith (2000)
L_2	2688 g cm^{-2}	Muon penetration depth	Granger and Smith (2000)
L_3	4360 g cm^{-2}	Fast muon penetration depth	Granger and Smith (2000)
P_n	5·1 atoms ^{10}Be g^{-1} a^{-1}	Nucleonic ^{10}Be production rate	Lal (1991), Stone (2000)
A_1	170·6 μ$^-$ g^{-1} a^{-1}	Muon production rate	Granger and Smith (2000)
A_2	36·75 μ$^-$ g^{-1} a^{-1}	Muon production rate	Granger and Smith (2000)
Y	5·6 × 10^{-4} atoms ^{10}Be/μ$^-$	^{10}Be yield per negative muon	Heisinger (1998)
B	0·026 atoms ^{10}Be g^{-1} a^{-1}	Fast muon ^{10}Be production rate	Granger and Smith (2000)
Other parameters			
d	1·5 ± 0·5 m	Soil depth	Assumed
ρ_s	1·5 ± 0·25 g cm^{-3}	Soil density	Assumed
f_s/f_r	1·04 ± 0·01	Soil quartz enrichment	Assumed*

Values listed for production constants P_n, Y, A_1, A_2, B are for sea level and high latitude, and are modified for the characteristics of each field site. Values for P_n are modified for latitude and altitude according to Lal (1991); P_n and Λ are modified for topographic shielding according to Masarik *et al.* (2000); YA_1, YA_2, and B are modified for altitude according to Stone *et al.* (1998); and P_n, YA_1, YA_2, B are modified to account for vegetative shielding as described in the text.

* Quartz enrichment in Redwood Creek soil is calculated as $W/D + 1$, where W is the chemical weathering rate (49·7 t km^{-2} a^{-1}; Dethier, 1986) and D is the total denudation rate (chemical weathering rate + physical erosion rate). We use the average 1971–2000 sediment yield at Redwood Creek at Orick (1304 ± 231 t km^{-2} a^{-1}) as the physical erosion rate. In the absence of chemical weathering rate data for Caspar Creek, we assume that quartz enrichment in Caspar Creek soil is the same as in Redwood Creek soil.

After determining ^{10}Be concentrations, we calculated denudation rates by iteratively solving Equation 1 (Granger *et al.*, 2001), which says that the total ^{10}Be concentration (N) is the sum of ^{10}Be concentrations due to nucleon spallation (the first term) and muogenic production (the last three terms):

$$N = \frac{P_n}{\tau^{-1} + \rho\varepsilon(\Lambda^{-1})} + \frac{YA_1}{\tau^{-1} + \rho\varepsilon(L_1^{-1})} + \frac{YA_2}{\tau^{-1} + \rho\varepsilon(L_2^{-1})} + \frac{B}{\tau^{-1} + \rho\varepsilon(L_3^{-1})} \tag{1}$$

where P_n is the production rate of ^{10}Be at the surface due to nucleon spallation, τ is the radioactive meanlife of ^{10}Be, ε is the denudation rate, ρ is the density of the quartz-bearing material (i.e. rock or soil), Λ is the penetration depth for nucleons, and L_1, L_2, and L_3 are the penetration depths for muon reactions. A_1 and A_2 are the production rates of negative muons in quartz, Y is the yield of ^{10}Be per negative muon, and B is the production rate of ^{10}Be due to fast (i.e. high energy) muons. For each sample site, we scaled P_n for latitude and altitude according to Lal (1991), P_n and Λ for topographic shielding according to Masarik *et al*. (2000), and muogenic production rates for altitude according to Stone *et al*. (1998). Values for the above parameters at sea level and high latitude are listed in Table II. In order to determine the mean production rate of ^{10}Be at each sample site, we calculated production rates across the range of elevations at each catchment and computed an areally weighted average production rate based on basin hypsometry. At our study catchments, production rates calculated in this manner differed from production rates at the mean basin elevation by at most 3 per cent. We scaled denudation rates to account for preferential weathering of minerals other than quartz, which increases the residence time of quartz in soil, and hence increases the exposure time of quartz grains to cosmogenic radiation (Small *et al*., 1999; Riebe *et al*., 2001). Denudation rates determined from Equation 1 are averaged over a characteristic timescale of $\Lambda\ \rho_{rock}^{-1}\ \varepsilon^{-1}$, the time required to erode a layer of rock *c*. 60 cm thick; the characteristic erosional timescale for each site is listed in Table I.

Accounting for vegetative shielding

Materials such as snow, ice and vegetation shield the Earth's surface from cosmic radiation and reduce the production rate of cosmogenic nuclides in the underlying soil and rock (e.g. Lal, 1991). In many regions, shielding due to vegetation is minimal (e.g. Brown *et al*., 1995), but above-ground biomass densities in the Northern California redwood forests are among the highest in the world (Waring and Franklin, 1979), so the ^{10}Be production rate P_n in Equation 1 must be modified accordingly. In order to estimate biomass density, we averaged six measurements of biomass volume from old-growth *Sequoia sempervirens* forests in the Northern California Coast Ranges (Westman and Whittaker, 1975; Fujimori, 1977), and assumed a live redwood bulk density of 800 kg m^{-3} (USDA, 1987). These estimates produce a vegetative mass density of 51 ± 13 g cm^{-2} (mean ± s.e.).

Pollen studies from an offshore sediment core (ODP Site 1019; 41·682° N, 124·930° W) suggest that Coast Range forests reached their current composition about 4000 years ago, and that *Sequoia sempervirens* was roughly half as common during the mid-Holocene (Barron *et al*., 2003). Assuming that this pollen record accurately reflects the vegetative history of our field sites, we estimate that the biomass density was 51 ± 13 g cm^{-2} from 4 ka to present, and half that prior to 4 ka. At Caspar Creek, the original forests were dominated by coast redwood, Douglas fir and grand fir (Reid and Hilton, 1998), while at Redwood Creek, 82 per cent of the basin is dominated by coast redwood and Douglas fir, and the remaining 18 per cent is split evenly between oak woodlands and grasslands (Best, 1995). We assume that the biomass density of 51 ± 13 g cm^{-2} is relevant to the entire Caspar Creek catchment, and that the spatially averaged biomass density at Redwood Creek is 82 per cent of that calculated above. These assumptions yield average biomass densities ranging from 38 to 45 g cm^{-2} at Caspar Creek and 41 to 42 g cm^{-2} at Redwood Creek. These biomass densities reduce the production rate of ^{10}Be to 75–79 per cent of its unshielded rate, and we applied these correction factors to our calculations for each field site.

Beryllium-10 sample preparation

Sample preparation followed the procedures outlined in Riebe (2000). We collected stream sediment samples from active bars in the stream channel away from obvious landslide deposits. Because of the low abundance of quartz at these field sites, we needed to process 5–6 kg of stream sediment in order to obtain the necessary 50–100 g of quartz for each sample. After crushing the sediment to a grain size of 0·25–0·5 mm, we isolated quartz via magnetic separation and chemical dissolution in hydrochloric, phosphoric, nitric, and hydrofluoric acids (Kohl and Nishiizumi, 1992). After verifying the purity of the quartz by measuring aluminium concentrations with inductively coupled plasma spectrophotometry, we spiked quartz samples with ^{9}Be carrier and dissolved the quartz in HF and HNO_3. The dissolved samples were then dried down in platinum crucibles, redissolved and dried down in H_2SO_4, raised to 1 N HCl solution, and passed through cation exchange columns. We then precipitated out titanium hydroxide by raising the solution to pH 5 and centrifuging the samples, and then extracted beryllium hydroxide from the remaining solution by raising the solution to pH 8 and centrifuging again. We then transferred the beryllium hydroxide to quartz crucibles and oxidized the samples at 750 °C. Lastly, we mixed the beryllium oxide samples with niobium powder, and packed the mixtures in target holders to be run at the Center for Accelerator Mass Spectrometry, Lawrence Livermore National Laboratory.

Sediment monitoring

Caspar Creek. Streamflow and suspended sediment concentration have been measured at the North Fork and South Fork of Caspar Creek since 1962 and at the North Fork tributaries since 1986 (Henry, 1998). Bedload accumulation is surveyed annually in the ponds behind the North Fork and South Fork weirs, and this volume is converted to mass based on a density of 1185 kg m^{-3} (Lewis, 1998). Approximately 40 per cent of the total sediment load settles in these weir ponds.

Suspended sediment sampling methods have changed since monitoring began, which is of concern because early sampling procedures may have produced biased estimates of sediment flux. Prior to 1975, suspended sediment fluxes may have been overestimated by a factor of two to three (Lewis, 1998), because calculations of suspended sediment load were based on empirical relationships between suspended sediment concentration and discharge, and most suspended sediment samples were collected on the rising limb of the hydrograph. Measurements during storms at Caspar Creek have since shown that suspended sediment concentrations are higher on the rising limb of the hydrograph than at equivalent discharges on the falling limb (Lewis, 1998). Calculated sediment loads, therefore, were overestimated to the degree that suspended sediment concentrations on the rising limb exceeded the mean suspended sediment concentration at equivalent discharges. Because 1963–1975 sediment loads were probably overestimated by a factor of two to three (Lewis, 1998), we arbitrarily scaled down Caspar Creek suspended sediment fluxes from 1963–1975 to 40 per cent of their originally documented values.

At the North Fork tributaries Carlson, Eagle, Henningson and Iverson, suspended sediment concentrations have been measured since 1986, but bedload fluxes have not. To calculate total sediment yields for these tributaries, we

Table III. Regression equations used to estimate suspended sediment loads at Caspar Creek tributaries Carlson, Eagle, Henningson and Iverson, based on 1986–2003 storm sediment loads at the North Fork and South Fork of Caspar Creek

Catchment	Regression equations used to estimate suspended load (tons)	R^2	*n**
Carlson	log(CAR) = −0·1280 + 0·9006 × log(NFC)	0·83	83
	log(CAR) = −0·2119 + 0·8636 × log(SFC)	0·70	80
Eagle	log(EAG) = −0·0407 + 1·0481 × log(NFC)	0·81	87
	log(EAG) = −0·1156 + 1·0257 × log(SFC)	0·67	86
Henningson	log(HEN) = −0·4016 + 1·0912 × log(NFC)	0·89	82
	log(HEN) = −0·6627 + 1·1320 × log(SFC)	0·82	79
Iverson	log(IVE) = −0·5610 + 0·9025 × log(NFC)	0·79	78
	log(IVE) = −0·6953 + 0·8852 × log(SFC)	0·73	74

Because Carlson, Eagle, Henningson and Iverson are tributaries of the North Fork, we applied a regression of tributary sediment load against North Fork load wherever possible. For storms without North Fork data, we applied a regression of tributary sediment load against South Fork load. Abbreviations stand for suspended sediment loads (in tons) at the following stations: NFC, North Fork Caspar Creek; SFC, South Fork Caspar Creek; CAR, Carlson; EAG, Eagle; HEN, Henningson; IVE, Iverson.
* Number of data points used to create the regression.

Table IV. Linear regression equations used to estimate bedload at Redwood Creek sites. Regressions are based upon annual suspended load and bedload measurements at each site

Catchment	Regression equation used to estimate bedload (tons)	R^2	*n**
Redwood Creek at Orick	bedload = 60 043 + 0·1275 × suspended load	0·52	19
Coyote Creek	bedload = 909 + 0·2906 × suspended load	0·85	8
Little Lost Man Creek	bedload = 49 + 0·2269 × suspended load	0·92	5
Panther Creek	bedload = 139 + 0·4596 × suspended load	0·62	11

* Number of years with both bedload and suspended load data, and also the number of data points used to create the regression equations.

assumed that the bedload fraction was the same as the 1989–1995 bedload fraction measured at the North Fork, i.e. 0·31 (J. Lewis, personal communication, October 2004). This is not an unreasonable assumption; grain size distributions probably do not change much in the short distance (<2·5 km) between the tributaries and the North Fork weir.

The suspended sediment yield records at these tributaries have many gaps. Suspended sediment yield data are tabulated by storm, where a 'storm' is defined as an event in which water levels exceed 2 feet (0·61 m) at the South Fork weir. In each tributary dataset, between 24 and 35 (out of 116) storms lack good quality suspended sediment data. Where possible, we estimated suspended sediment yields for 'missing' data using log-linear regressions of tributary suspended sediment yields against North Fork and South Fork suspended sediment yields. These regressions are listed in Table III. Suspended sediment yields could not be estimated in this manner for three storms because every gauging station lacked good quality data. However, these three storms were probably small (J. Lewis, personal communication, 2004), and we assume they did not significantly contribute to the total sediment flux over the 18 years of record.

Redwood Creek. At Orick, near the mouth of Redwood Creek, stream sediment fluxes have been measured since 1971, first under the USGS and later under Redwood National Park and Redwood State Park. The tributaries of Redwood Creek considered in this study have between 13 and 20 years of suspended sediment data. The sediment yield records are not continuous: between 1 and 3 years of data are missing from each of the tributary records, and bedload was not recorded later than 1992. For years without bedload data, we estimated bedload as a function of suspended load by creating linear regressions of bedload against suspended load for each station. These regression equations are listed in Table IV.

Results

Beryllium-10 measurements and calculated denudation rates

Table I lists all ^{10}Be concentrations and calculated denudation rates for Caspar Creek and Redwood Creek. At Caspar Creek, millennial-scale denudation rates at each basin nearly agree within error, and average 0·09 ± 0·02 mm a^{-1}. Millennial-scale denudation rates at Redwood Creek vary by a factor of 3, from 0·14 ± 0·03 mm a^{-1} at Little Lost Man Creek to 0·44 ± 0·09 mm a^{-1} at Redwood Creek at Orick.

Decadal-scale sediment yields

Caspar Creek. By summing annual suspended sediment yields and bedload yields (RSL website, 2004), and scaling sediment yields by an assumed bedrock density of 2700 kg m^{-3}, we calculated total 1963–2002 erosion rates for the North Fork and South Fork of Caspar Creek to be 0·057 ± 0·015 mm a^{-1} and 0·064 ± 0·012 mm a^{-1} (mean ± s.e.), respectively. Multiplying the 1963–1975 suspended sediment yields by a factor of 0·4 to account for sampling bias, as described above, reduces the total erosion rates for the North Fork and South Fork of Caspar Creek to 0·044 ± 0·009 mm a^{-1} and 0·046 ± 0·007 mm a^{-1} (mean ± s.e.), respectively. We assume that these rescaled estimates more closely represent actual 1963–2002 erosion rates. At the tributaries Carlson, Eagle, Henningson and Iverson, assuming that the storm records capture 100 per cent of the suspended sediment flux, and that the bedload flux at these tributaries is 0·31 of the total sediment flux, erosion rates range from 0·005 ± 0·001 mm a^{-1} to 0·037 ± 0·011 mm a^{-1} (Table V).

Redwood Creek. We calculated Redwood Creek sediment yields as the sum of suspended sediment yield and bedload yield. Mean annual sediment yields over the past few decades are generally higher than decadal-scale Caspar Creek sediment yields, and are highly variable from basin to basin. The mean 1971–2000 sediment yield for Redwood Creek at Orick, for example, is 12 times higher than the mean 1985–2000 sediment yield at Little Lost Man Creek (Table V).

Table V. Summary of sediment monitoring results at Caspar Creek and Redwood Creek

Catchment	Years of record: Suspended load	Years of record: Bedload	Sediment yield (t km^{-2} a^{-1}) (mean ± s.e.)*	Erosion rate (mm a^{-1}) (mean ± s.e.)†	Ratio of rates‡
Caspar Creek					
North Fork	1963–2002	1963–2002	119 ± 25	0·044 ± 0·009	2·4
South Fork	1963–2002	1963–2002	125 ± 18	0·046 ± 0·007	1·5
Carlson	1986–2003	–	27 ± 6	0·010 ± 0·002	10·1
Eagle	1986–2003	–	99 ± 31	0·037 ± 0·011	1·9
Henningson	1986–2003	–	45 ± 12	0·017 ± 0·004	6·1
Iverson	1986–2003	–	12 ± 3	0·005 ± 0·001	16·0
Redwood Creek					
Redwood Creek at Orick	1971–2000	1974–1992	1304 ± 231	0·48 ± 0·09	0·9
Coyote Creek	1980–1982, 1984–1988, 1992–1995	1980–1988	1112 ± 414	0·41 ± 0·15	0·4
Little Lost Man Creek	1985–1989, 1993–2000	1985–1989	103 ± 29	0·038 ± 0·011	3·6
Panther Creek	1980–1990, 1992–2000	1980–1990	383 ± 160	0·14 ± 0·06	1·6

Sediment yield measurements at Caspar Creek were collected by Pacific Southwest Research Station, Redwood Sciences Laboratory and the California Department of Fire and Forestry Protection. Sediment yield measurements at Redwood Creek were collected by the US Geological Survey, Redwood National Park and Redwood State Park.

* Sediment yields include assumed bedload fractions for years lacking bedload measurements.

† Erosion rates are calculated from sediment yields based on an assumed bedrock density of 2700 kg m^{-3}.

‡ 'Ratio of rates' is the millennial-scale denudation rate (derived from ^{10}Be measurements; see Table I) divided by the decadal-scale erosion rate derived from measurements of stream sediment flux over the past several decades.

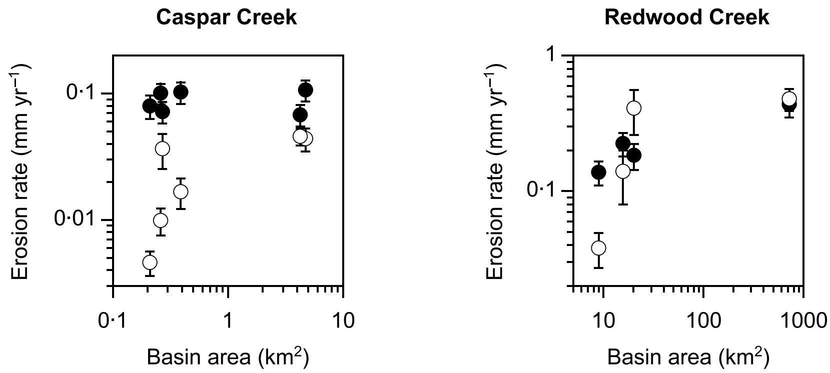

Figure 2. Erosion rates at Caspar Creek and Redwood Creek, averaged over millennial timescales (filled circles) and over decadal timescales (open circles). Uncertainties are one standard error.

Assuming a bedrock density of 2700 kg m^{-3}, Redwood Creek sediment yields translate to erosion rates ranging between $0{\cdot}038 \pm 0{\cdot}011$ mm a^{-1} and $0{\cdot}48 \pm 0{\cdot}09$ mm a^{-1}.

Discussion

Comparison of millennial-scale and decadal-scale erosion rates

The denudation rates we measured over millennial timescales by cosmogenic ^{10}Be are less spatially variable, and have smaller uncertainties, than erosion rates inferred from sediment yield measurements over decadal timescales. Our ^{10}Be measurements imply that over the past *c*. 5500–8700 years (Table I), Caspar Creek has experienced denudation rates that are nearly spatially uniform across the entire catchment, and average $0{\cdot}09 \pm 0{\cdot}02$ mm a^{-1} (Figure 2). By comparison, erosion rates derived from post-1962 sediment yields are slower than millennial-scale denudation rates, and show more spatial variability, ranging from *c*. 0·005 mm a^{-1} up to *c*. 0·05 mm a^{-1}. In general, the smallest basins show the greatest discrepancy between decadal-scale and millennial-scale measurements (Figure 2).

At Redwood Creek, denudation rates implied by ^{10}Be vary by a factor of three from basin to basin, ranging from $0{\cdot}14 \pm 0{\cdot}03$ mm a^{-1} to $0{\cdot}44 \pm 0{\cdot}09$ mm a^{-1} over the past *c*. 1400–4300 years (Table I). Erosion rates inferred from decadal-scale sediment yields range from *c*. 0·04 mm a^{-1} to *c*. 0·48 mm a^{-1} and agree with millennial-scale denudation rates within error at Panther Creek and Redwood Creek at Orick, but the decadal-scale rate is about twice a fast as the millennial-scale rate at Coyote Creek and 3·6 times slower at Little Lost Man Creek (Figure 2).

Could the calculated rates be wrong?

Is it possible that the decadal-scale sediment yield measurements are too low or the ^{10}Be-derived denudation rates are too high? The fact that ^{10}Be measurements reflect total denudation (physical erosion + chemical weathering fluxes) while sediment gauging records reflect only physical erosion should not cause a large difference between the millennial-scale and decadal-scale rates documented here. Previous measurements at Redwood Creek indicate that chemical denudation rates (49·7 t km^{-2} a^{-1}; Dethier, 1986) constitute a small fraction of the total denudation rates measured in this study (1149 ± 226 t km^{-2} a^{-1}). Cosmogenic rates could also be too high if the parameters used in the calculations are wrong. For example, at each site we assumed the soil had an average density of $1{\cdot}5 \pm 0{\cdot}25$ g cm^{-3} and an average depth of $1{\cdot}5 \pm 0{\cdot}5$ m. Changing each of these parameters by a factor of two, however, changes calculated denudation rates by less than 5 per cent. We also assumed that quartz enrichment in the soil relative to bedrock (e.g. Small *et al*., 1999; Riebe *et al*., 2001) is 4 per cent; decreasing this enrichment to 0 per cent reduces millennial-scale denudation rates by only 2 per cent. It is also important to consider potential biases due to grain size effects, since some studies (e.g. Brown *et al*., 1995) have found a correlation between grain size and ^{10}Be concentrations, where larger grains, delivered to the stream by landslides, have lower concentrations of ^{10}Be. Most of our stream sediment samples were dominated by relatively large grains; at Caspar Creek, grains larger than 2 mm constituted 72–88 per cent of our sediment sample, and at Redwood Creek, grains larger than 2 mm constituted 18–69 per cent of our sediment samples. This should bias our calculated denudation rates if grain size is correlated with exposure to cosmogenic radiation at our field sites, and if the grain size distribution of our sediment samples deviates from the average distribution of grain sizes in stream sediment at our field sites. If our sediment samples have abnormally large grains with abnormally low ^{10}Be concentrations, then actual denudation rates would be lower than our calculated denudation rates.

Decadal-scale erosion rates could be too low if the sediment gauging stations missed part of the sediment flux. However, it seems unlikely that gauging inefficiency could account for the discrepancy between the decadal-scale and millennial-scale measurements (J. Lewis, personal communication, 2004). At Caspar Creek, gauging stations would have to miss 37–94 per cent of the sediment flux in order to match millennial-scale rates. Decadal-scale sediment yields at tributaries Carlson, Eagle, Henningson and Iverson might also be too low if the assumed bedload fraction were too low. At these tributaries, however, bedload would have to constitute 66–96 per cent of the total load in order to account for the discrepancy, which is inconsistent with the observation that only *c*. 30 per cent of the total yield accumulates as bedload in the weir ponds.

How has logging affected ^{10}Be concentrations in our stream sediment samples?

Clear-cut logging at Caspar Creek from 1860 to 1906 (Henry, 1998) probably led to rapid erosion, which implies that ^{10}Be concentrations in our sediment samples might be lower than they would have been if the study catchments had never been logged. If this is the case, then our calculated denudation rates would be faster than actual millennial-scale denudation rates. Unfortunately, since we are not aware of estimates of erosion rates during the 19th century, it is not possible to properly account for this in the denudation rate calculation. Nonetheless, we suspect that our calculated denudation rates are not far from actual millennial-scale denudation rates, since ^{10}Be concentrations are fairly insensitive to recent changes in denudation rates. For example, if clear-cut logging during the years 1860–1906 had uniformly eroded 100 cm of soil (that is, if erosion rates had been *c*. 500 times faster than 1963–2002 erosion rates at the North Fork of Caspar Creek), then our calculated denudation rates would overestimate the pre-logging denudation rate by only about a factor of two. As a rough comparison, Lewis (1998) calculated that erosion rates were elevated by less than a factor of three at the South Fork of Caspar Creek during 1972–1978, the period which immediately followed removal of *c*. 65 per cent of the South Fork stand volume. Thus 1860–1906 erosion rates would have to have been very high in order to drastically alter the ^{10}Be concentrations in our sediment samples.

What causes the observed spatial variation in erosion rates?

The spatial similarity in millennial-scale denudation rates across the Caspar Creek basin is not surprising, given that the underlying lithology varies little throughout the basin (Jennings and Strand, 1960), hillslope gradients are roughly the same in each tributary basin (Table I), and the small size (*c*. 9 km^2) of the study area makes for a roughly uniform climate. The small spatial variability in ^{10}Be concentrations suggests that erosion rates, when averaged over a sufficiently long time period, approach a single constant rate throughout the Caspar Creek catchment. This small spatial variability in ^{10}Be concentrations contrasts with the large spatial variability in the decadal-scale measurements, suggesting that erosional processes at Caspar Creek vary on timescales longer than decades and shorter than the cosmogenic erosional timescale, i.e. <5500 years (Table I).

According to our Redwood Creek ^{10}Be measurements, Coyote Creek, Panther Creek and Little Lost Man Creek are eroding more slowly than Redwood Creek basin as a whole, implying that the unsampled tributaries of Redwood Creek must be eroding more quickly, on average, than the three tributaries we sampled. It would not be surprising to find that the fastest erosion rates are concentrated farther south than the tributaries we sampled, since Redwood Creek is much steeper near its southernmost headwaters, and the higher elevations there may be subject to enhanced physical weathering due to more intense freeze–thaw cycles. Mean hillslope gradients vary little from site to site (Table I), and so are probably not the main cause of variation in denudation rates. Lithology has been shown to regulate bedrock river incision rates (e.g. Sklar and Dietrich, 2001), but its influence on hillslope denudation rate is not apparent in our ^{10}Be measurements. For example, Coyote Creek cuts through incoherent sandstone and mudstone, and Panther Creek incises the Redwood Creek Schist (Harden *et al*., 1981), yet their millennial-scale denudation rates agree with each other within error. This agreement in denudation rates at Panther Creek and Coyote Creek might be a result of main stem forcing, since these tributaries enter the main stem of Redwood Creek at about the same location (Figure 1). If the morphologies of Panther Creek and Coyote Creek are both adjusted to produce incision rates that match Redwood Creek's incision rate, then the steepness of these tributaries should reflect differences in bedrock strength – that is, the tributary in the stronger lithology should be steeper than the tributary in the weaker lithology. However, the mean channel gradient at Coyote Creek is *c*. 0·12, and at Panther Creek it is *c*. 0·08 (Figure 3). This would seem to suggest

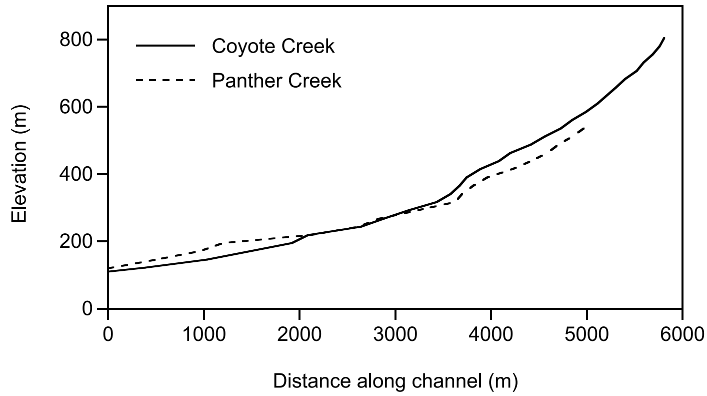

Figure 3. Longitudinal profiles of Coyote Creek and Panther Creek, determined from 1:24 000 USGS topographic maps. The horizontal axis is distance from the main stem of Redwood Creek, measured along the channel. Mean channel gradients are *c.* 0·12 at Coyote Creek and *c.* 0·08 at Panther Creek.

that, if the difference in channel gradient were purely a function of differences in lithologic strength, then the incoherent sandstone underlying Coyote Creek would be stronger than the Redwood Creek Schist underlying Panther Creek, which is implausible. Thus any influence of bedrock lithology on hillslope denudation rates is not evident in our cosmogenic ^{10}Be measurements. Measurements of bedrock tensile strength, as well as further ^{10}Be measurements from stream sediment in other tributaries, could help quantify the influence of lithology on erosion rates in the Redwood Creek basin.

In the decadal-scale measurements, the spatial differences in erosion rates appear to be partially attributable to the different measurement periods. At Caspar Creek, the records for tributaries Carlson, Eagle, Henningson and Iverson span 1986–2003, while the North Fork and South Fork records go back to 1963. The mean 1986–2002 erosion rates at the North Fork and South Fork are $0{\cdot}029 \pm 0{\cdot}008$ mm a^{-1} and $0{\cdot}039 \pm 0{\cdot}011$ mm a^{-1} (mean ± s.e.) respectively; this is slower than the mean 1963–2002 North Fork and South Fork erosion rates, but still faster than most of the 1986–2003 tributary erosion rates. Similarly, during the monitoring periods at Coyote Creek, Panther Creek and Little Lost Man Creek (Table V), the average physical erosion rate at Redwood Creek at Orick ranged from $0{\cdot}32 \pm 0{\cdot}07$ mm a^{-1} to $0{\cdot}36 \pm 0{\cdot}06$ mm a^{-1} (mean ± s.e.), which is slower than the 1971–2000 erosion rate of $0{\cdot}48 \pm 0{\cdot}09$ mm a^{-1} (mean ± s.e.) at Redwood Creek at Orick, but still faster than erosion rates at Panther Creek and Little Lost Man Creek. These calculations suggest that, within the Caspar Creek and Redwood Creek catchments, the site-to-site differences in the decadal-scale measurements are partially, but not entirely, due to the different measurement periods.

What causes the observed temporal variation in erosion rates?

Why are there discrepancies between the decadal-scale and millennial-scale erosion rates at some of the basins and not in others? It should be noted that at most of the study basins, the difference between decadal-scale and millennial-scale erosion rates is a factor of two to three, which is not particularly large. A similar study in Idaho (Kirchner *et al.*, 2001) found that millennial-scale denudation rates were, on average, 17 times faster than short-term erosion rates, most likely reflecting extremely episodic sediment delivery to streams. Another study in Sri Lanka (Hewawasam *et al.*, 2003) found the opposite: short-term erosion rates that were an order of magnitude faster than denudation rates averaged over the past *c.* 20 000 years, reflecting recent human disturbance. A potential explanation for the difference in erosion rates at Caspar Creek and Redwood Creek is that sediment delivery to streams is naturally episodic; it is possible that the past 40 years of sediment monitoring have seen relatively few of the large events that dominate long-term average erosion rates.

Why do the smallest catchments tend to have slower decadal-scale rates?

Especially at Caspar Creek, it appears that small catchments show greater disparity between millennial-scale and decadal-scale sediment yields than large catchments. This observation is consistent with the hypothesis that small catchments are dominated by episodic sediment delivery. That is, if sediment delivery from small catchments is usually slow, and is infrequently punctuated by large events (e.g. landslides, debris flows), then the decadal-scale sediment yield in small basins will usually be low and infrequently high. At the mouth of a large basin, on the other hand, the sediment yield is the average of all the sediment yields from the upstream tributaries. If the tributary basins are dominated by episodic sediment delivery, and if the timing of sediment delivery were uncorrelated from one tributary to another, then the decadal-scale sediment yield at a large basin would be the average of many low sediment yields and a few high sediment yields. This averaging could result in a sediment yield at a large basin that is higher than the low sediment yields experienced by most of the small tributary basins in any particular period, yet still lower than the long-term average sediment yield in the large basin. If millennial-scale erosion rates are dominated by episodic erosion, then over a short time period the spatial pattern of sediment yields could match the pattern of decadal-scale sediment yields observed at Caspar Creek (Figure 2).

How would the spatial pattern of erosion be interpreted if we only had the decadal-scale sediment yields?

The spatial patterns of erosion revealed by the decadal-scale and millennial-scale measurements are quite different, and highlight the value of using cosmogenic denudation rate measurements in landscape evolution models. Decadal-scale sediment fluxes suggest that erosion rates vary in space by a factor of 10 at Caspar Creek and a factor of 12 at Redwood Creek, while our cosmogenic ^{10}Be measurements suggest that erosion rates are nearly spatially uniform at Caspar Creek and vary by a factor of three at Redwood Creek. Because the decadal-scale sediment fluxes imply greater spatial variability in erosion rates than our cosmogenic ^{10}Be measurements imply, the decadal-scale rates would be interpreted as predicting greater variability in landscape morphology over time. However, because the cosmogenic denudation rates are averaged over longer timescales than the sediment flux measurements at Caspar Creek and Redwood Creek, denudation rates determined from measurements of cosmogenic ^{10}Be are more likely to be representative of the processes that dominate long-term landscape evolution.

How do these denudation rates compare with uplift rates?

Many researchers have posited that landscapes tend to approach topographic steady state, a condition in which a particular property of the landscape (e.g. mean elevation) remains constant over time (e.g. Hack, 1960; Willett and Brandon, 2002). In such a situation, if a region is undergoing spatially uniform uplift, erosion rates are also spatially uniform. Caspar Creek is an example of a landscape that is undergoing nearly spatially uniform erosion over millennial timescales, but which is not eroding as quickly as it is being uplifted. Ages and elevations of nearby marine terraces yield uplift rates of 0·3–0·4 mm a^{-1} (Kennedy *et al*., 1982; Merritts and Bull, 1989), higher than both the millennial-scale and decadal-scale erosion rates at Caspar Creek. If this uplift rate is also the mean uplift rate over the timescale of our cosmogenic denudation rates, our ^{10}Be measurements indicate that the mean elevation of Caspar Creek has been increasing at an average rate of *c*. 0·2–0·3 mm a^{-1}.

The marine terrace ages also reveal that our catchment-averaged denudation rates do not agree with the rate of river incision through the terraces in lower Caspar Creek. The oldest marine terrace to which Merritts and Bull (1989) assigned an age is the *c*. 130 m terrace, which they correlated with the 330 ka sea-level highstand. Next to this terrace, Caspar Creek has an elevation of *c*. 10 m, which implies that Caspar Creek has incised through *c*. 120 m in 330 ka – an incision rate of 0·36 mm a^{-1}. There are several possible reasons why this river incision rate does not match the average denudation rate of 0·09 ± 0·02 mm a^{-1} implied by our ^{10}Be measurements. First, the 130 m terrace is downstream of our ^{10}Be sampling locations, so it is possible that erosion rates in lower Caspar Creek are faster than in upper Caspar Creek. Second, it is possible that the difference is due to the different timescales; the rate of river incision through the terrace is a 330 ka average, while the ^{10}Be-derived denudation rates are *c*. 5–9 ka averages (Table I). It might be that Caspar Creek has simply eroded more slowly over the past *c*. 5–9 ka than it has over the past 330 ka. Third, it is possible that the river incision rate is faster than the hillslope denudation rate. Fourth, it is possible that the ages Merritts and Bull (1989) assigned to the terraces are too young. Aside from the 24 m terrace, which was dated using amino-acid racemization (Kennedy *et al*., 1982; Lajoie *et al*., 1991), all terrace ages near Caspar Creek were assigned by correlating terraces to sea-level highstands of known age (Merritts and Bull, 1989). Elsewhere in California, cosmogenic dating of marine terraces (Perg *et al*., 2001) has yielded ages that differ from those determined by sea-level correlation. This suggests that the older marine terraces near Caspar Creek might have significantly different ages than those reported in Merritts and Bull (1989), and implies that the uplift rate estimates should be treated with caution. If the 130 m terrace were *c*. 1·4 million years old instead of 330 ka, the calculated rock uplift rate would match our cosmogenic denudation rate of 0·09 ± 0·02 mm a^{-1}. Assuming the terrace ages assigned by Merritts and Bull (1989) are correct, the denudation rates in upper Caspar Creek over the past 5–9 ka are slower than both the average river incision rate in lower Caspar Creek and the average rock uplift rate over the past 330 ka.

Conclusions

Our measurements of ^{10}Be in stream sediment imply that, at most of the basins examined in this study, millennial-scale denudation rates are in rough agreement with, or somewhat higher than, sediment yields measured over the past few decades. At Caspar Creek millennial-scale denudation rates tend to be faster, relative to decadal-scale rates, than at Redwood Creek; millennial-scale measurements are 1·5–16 times as fast as decadal-scale measurements at Caspar Creek, and 0·4–3·6 times as fast at Redwood Creek.

In addition, millennial-scale and decadal-scale erosion rates tend to show large discrepancies over small catchments and small discrepancies over larger catchments (i.e. at North Fork Caspar Creek, South Fork Caspar Creek, Redwood Creek at Orick). In contrast to order-of-magnitude differences found elsewhere (e.g. Kirchner *et al*., 2001; Hewawasam *et al*., 2003), the sediment yields measured over the past few decades at the mouths of Caspar Creek and Redwood Creek differ from millennial-scale rates of sediment production by less than a factor of three.

These measurements also imply that, within these two catchments, there is greater spatial variability in erosion rates over decadal timescales than over millennial timescales. At Caspar Creek, sediment yields measured over the past few decades vary by nearly an order of magnitude from site to site, but ^{10}Be measurements imply nearly spatially uniform denudation rates over the past *c*. 5–9 ka. At Redwood Creek, decadal-scale sediment yields differ in space by a factor of 12, while millennial-scale denudation rates inferred from cosmogenic ^{10}Be measurements differ by a factor of three. This greater spatial variability over short timescales might be a reflection of episodic erosion.

Lastly, previous estimates of marine terrace ages and elevations near Caspar Creek (Merritts and Bull, 1989) indicate that rock uplift rates are substantially faster than denudation rates, implying that the mean elevation of Caspar Creek is rising at an average rate of 0·2–0·3 mm a^{-1}. This suggests that spatially uniform denudation rates, such as those observed at Caspar Creek, are not necessarily indicative of topographic steady state.

Acknowledgments

This manuscript benefited from the insightful comments of two anonymous reviewers. We thank Elizabeth Keppeler for access to field sites at Caspar Creek, Robert Ziemer, Jack Lewis and Leslie Reid for Caspar Creek sediment gauging records and helpful discussions, Mary Ann Madej and Randy Klein for Redwood Creek sediment gauging records, Simpson Resource Company and Andrew Frazier for access to field sites at Redwood Creek, Kate Barton for field assistance, and Cliff Riebe for laboratory instruction and helpful discussions. This work was partly supported by the National Council for Air and Stream Improvement and NSF grant EAR-0004098, and was performed under the auspices of the US Department of Energy by the University of California, Lawrence Livermore National Laboratory under Contract No. W-7405-Eng-48.

References

Barron JA, Heusser L, Herbert T, Lyle M. 2003. High-resolution climatic evolution of coastal northern California during the past 16,000 years. *Paleoceanography* **18**(1), 1020. DOI: 10.1029/2002PA000768.

Best DW. 1995. *History of timber harvest in the Redwood Creek basin, northwestern California*. USGS Professional Paper 1454-C.

Bierman P, Steig EJ. 1996. Estimating rates of denudation using cosmogenic isotope abundances in sediment. *Earth Surface Processes and Landforms* **21**: 125–139.

Brown ET, Stallard RF, Larsen MC, Raisbeck GM, Yiou F. 1995. Denudation rates determined from the accumulation of in situ-produced ^{10}Be in the Luquillo Experimental Forest, Puerto Rico. *Earth and Planetary Science Letters* **129**: 193–202.

Brown ET, Stallard RF, Larsen MC, Bourlès DL, Raisbeck GM, Yiou F. 1998. Determination of predevelopment denudation rates of an agricultural watershed (Cayaguás River, Puerto Rico) using in-situ-produced ^{10}Be in river-borne quartz. *Earth and Planetary Science Letters* **160**: 723–728.

Dethier DP. 1986. Weathering rates and chemical fluxes from catchments in the Pacific Northwest U.S.A. In *Rates of Chemical Weathering of Rocks and Minerals*, Coleman SM, Dethier DP (eds). Academic Press: New York; 503–530.

Fujimori T. 1977. Stem biomass and structure of a mature sequoia sempervirens stand on the Pacific coast of Northern California. *Journal of Japanese Forest Research* **59**: 435–441.

Granger DE, Smith AL. 2000. Dating buried sediments using radioactive decay and muogenic production of ^{26}Al and ^{10}Be. *Nuclear Instruments and Methods in Physics Research B* **172**: 822–826.

Granger DE, Kirchner JW, Finkel R. 1996. Spatially averaged long-term erosion rates measured from in situ-produced cosmogenic nuclides in alluvial sediment. *Journal of Geology* **104**: 249–257.

Granger DE, Riebe CS, Kirchner JW, Finkel RC. 2001. Modulation of erosion on steep granitic slopes by boulder armoring, as revealed by cosmogenic ^{26}Al and ^{10}Be. *Earth and Planetary Science Letters* **186**: 269–281.

Hack JT. 1960. Interpretation of erosional topography in humid temperature regions. *American Journal of Science* **258A**: 80–97.

Harden DR, Kelsey HM, Morrison SD, Stephens TA. 1981. Geologic map of the Redwood Creek drainage basin, Humboldt County, California. USGS Open-File Report 81-496.

Heimsath AM, Dietrich WE, Nishiizumi K, Finkel RC. 1997. The soil production function and landscape equilibrium. *Nature* **388**: 358–361.

Heisinger BP. 1998. *Myonen-induzierte Produktion von Radionukliden*. PhD thesis, Technische Universität München.

Henry N. 1998. Overview of the Caspar Creek watershed study. In *Proceedings of the Conference on Coastal Watersheds: The Caspar Creek Story*. General Technical Report PSW-GTR-168. Pacific Southwest Research Station, Forest Service, US Department of Agriculture: 1–9.

Hewawasam T, von Blanckenburg F, Schaller M, Kubik P. 2003. Increase of human over natural erosion rates in tropical highlands constrained by cosmogenic nuclides. *Geology* **31**(7): 597–600.

Iwatsubo RT, Nolan KM, Harden DR, Glysson GD, Janda RJ. 1975. *Redwood National Park studies, data release number 1, Redwood Creek, Humboldt County, California, September 1, 1973–April 10, 1974*. US Geological Survey Open-File Report.

Jennings CW, Strand RG. 1960. *Geologic map of California, Ukiah sheet, 1:250,000*. State of California Department of Natural Resources, Division of Mines.

Kennedy GL, Lajoie KR, Wehmiller JF. 1982. Aminostratigraphy and faunal correlations of late Quaternary marine terraces, Pacific Coast, U.S.A. *Nature* **299**: 545–547.

Kirchner JW, Finkel RC, Riebe CS, Granger DE, Clayton JL, King JG, Megahan WF. 2001. Mountain erosion over 10 yr, 10 k.y., and 10 m.y. time scales. *Geology* **29**(7): 591–594.

Kohl CP, Nishiizumi K. 1992. Chemical isolation of quartz for measurement of in-situ-produced cosmogenic nuclides. *Geochimica et Cosmochimica Acta* **56**: 3583–3587.

Lajoie KR, Ponti DJ, Powell II CL, Mathieson SA, Sarna-Wojcicki AM. 1991. Emergent marine strandlines and associated sediment, coastal California; A record of Quaternary sea-level fluctuations, vertical tectonic movements, climatic changes, and coastal processes. In *Quaternary Nonglacial Geology: Conterminous United States*. Geological Society of America, Geology of North America, K-2: 190–214.

Lal D. 1991. Cosmic ray labeling of erosion surfaces: in situ production rates and erosion models. *Earth and Planetary Science Letters* **104**: 424–439.

Lewis J. 1998. Evaluating the impacts of logging activities on erosion and suspended sediment transport in the Caspar Creek watersheds. In *Proceedings of the Conference on Coastal Watersheds: The Caspar Creek Story*. General Technical Report PSW-GTR-168. Pacific Southwest Research Station, Forest Service, US Department of Agriculture: 55–69.

Madej MA. 1995. *Changes in channel-stored sediment, Redwood Creek, northwestern California, 1947 to 1980*. USGS Professional Paper 1454-O.

Madej MA. 2001. Erosion and sediment delivery following removal of forest roads. *Earth Surface Processes and Landforms* **26**: 175–190.

Marron DC, Nolan M, Janda RJ. 1995. *Surface erosion by overland flow in the Redwood Creek basin, northwestern California – Effects of logging and rock type*. USGS Professional Paper 1454-H.

Masarik J, Reedy RC. 1995. Terrestrial cosmogenic-nuclide production systematics calculated from numerical simulations. *Earth and Planetary Science Letters* **136**: 381–395.

Masarik J, Kollar D, Vanya S. 2000. Numerical simulation of in situ production of cosmogenic nuclides: Effects of irradiation geometry. *Nuclear Instruments and Methods in Physics Research B* **172**: 786–789.

Merritts D, Bull WB. 1989. Interpreting Quaternary uplift rates at the Mendocino triple junction, northern California, from uplifted marine terraces. *Geology* **17**: 1020–1024.

Merritts D, Vincent KR. 1989. Geomorphic response of coastal streams to low, intermediate, and high rates of uplift, Mendocino triple junction region, northern California. *Geological Society of America Bulletin* **101**: 1373–1388.

Middleton R, Brown L, Dezfouly-Arjomandy B, Klein J. 1993. On ^{10}Be standards and the half-life of ^{10}Be. *Nuclear Instruments and Methods in Physics Research B* **82**: 399–403.

Napolitano MB. 1998. Persistence of historical logging impacts on channel form in mainstem North Fork Caspar Creek. In *Proceedings of the Conference on Coastal Watersheds: The Caspar Creek Story*. General Technical Report PSW-GTR-168. Pacific Southwest Research Station, Forest Service, US Department of Agriculture: 97–101.

Nolan KM, Janda RJ. 1995. *Impacts of logging on stream-sediment discharge in the Redwood Creek basin, northwestern California*. USGS Professional Paper 1454-L.

Perg LA, Anderson RS, Finkel RC. 2001. Use of a new ^{10}Be and ^{26}Al inventory method to date marine terraces, Santa Cruz, California, USA. *Geology* **29**(10): 879–882.

Pitlick J. 1995. *Sediment routing in tributaries of the Redwood Creek basin, northwestern California*. USGS Professional Paper 1454-K.

Reid LM, Hilton S. 1998. Buffering the buffer. In *Proceedings of the Conference on Coastal Watersheds: The Caspar Creek Story*. General Technical Report PSW-GTR-168. Pacific Southwest Research Station, Forest Service, US Department of Agriculture: 71–80.

Riebe CS. 2000. *Tectonic and climatic control of physical erosion rates and chemical weathering rates in the Sierra Nevada, California: inferred from cosmogenic nuclides and geochemical mass balance*. PhD thesis, University of California, Berkeley.

Riebe CS, Kirchner JW, Granger DS. 2001. Quantifying quartz enrichment and its consequences for cosmogenic measurements of erosion rates from alluvial sediment and regolith. *Geomorphology* **40**: 15–19.

Riebe CS, Kirchner JW, Finkel RC. 2003. Long-term rates of chemical weathering and physical erosion from cosmogenic nuclides and geochemical mass balance. *Geochimica et Cosmochimica Acta* **67**(22): 4411–4427.

RSL website 2004. USDA Forest Services, Pacific Southwest Research Station, Redwood Sciences Laboratory http://www.fs.fed.us/psw/topics/water/caspar [April, June 2004].

Sklar LS, Dietrich WE. 2001. Sediment and rock strength controls on river incision into bedrock. *Geology* **29**(12): 1087–1090.

Small EE, Anderson RS, Hancock GS. 1999. Estimates of the rate of regolith production using ^{10}Be and ^{26}Al from an alpine hillslope. *Geomorphology* **27**: 131–150.

Stone JO. 2000. Air pressure and cosmogenic isotope production. *Journal of Geophysical Research* **105**(B10): 23753–23759.

Stone JO, Evans JM, Fifield LK, Allan GL, Cresswell RG. 1998. Cosmogenic chlorine-36 production in calcite by muons. *Geochimica et Cosmochimica Acta* **62**(3): 433–454.

USDA. 1987. *Wood Handbook: Wood as an Engineering Material*. Agriculture Handbook 72. Forest Products Laboratory, US Department of Agriculture.

Waring RH, Franklin JF. 1979. Evergreen coniferous forests of the Pacific Northwest. *Science* **204**: 1380–1386.

Westman WE, Whittaker RH. 1975. The pygmy forest region of northern California: Studies on biomass and primary productivity. *Ecological Monographs* **63**: 493–520.

Willett SD, Brandon MT. 2002. On steady states in mountain belts. *Geology* **30**(2): 175–178.

WRCC website 2004. Western Regional Climate Center. http://www.wrcc.dri.edu [June 2004].

